Biogeochemistry (2025) 168:47
https://doi.org/10.1007/s10533-025-01237-4

Optical transformation of riverine colored dissolved organic matter during salt-induced flocculation

Eero Asmala · Ryan W. Paerl · Christopher L. Osburn

Received: 1 November 2024 / Accepted: 22 April 2025
© The Author(s) 2025

Abstract Flocculation of riverine dissolved organic matter (DOM) in estuaries is crucial for transforming and removing terrestrial carbon inputs across the land-to-ocean aquatic continuum. We measured variations in chromophoric DOM (CDOM) absorption and fluorescence of riverine DOM through mixing experiments conducted across various seasons and environments, identifying patterns in salt-induced flocculation. Our observations show a systematic reduction in CDOM absorption in the 250–450 nm range at salinity 2, with a sharper decrease at higher wavelengths. Flocculation led to decreased relative fluorescence intensity below emission wavelength of 360 nm and an increased intensity at higher emission wavelengths across the excitation spectrum measured (250–450 nm). We introduce a new metric, *red shift ratio*, a fluorescence-based metric calculated as the ratio of emission intensity at 300–350 nm to that at 360–500 nm, at excitation wavelengths between 250 and 300 nm, for detecting flocculation-induced changes in CDOM across estuarine systems. The observed sensitivity of CDOM to flocculation in low salinities challenges its use as a conservative tracer in coastal gradients, suggesting that recalibrations are required for remote sensing algorithms and carbon flux estimations across land-sea continuum, particularly in systems with similar characteristics.

Keywords Estuaries · Land-sea continuum · Terrestrial carbon input · Optical fingerprint · Absorption · Fluorescence

Responsible Editor: Stephen D. Sebestyen.

Supplementary Information The online version contains supplementary material available at https://doi.org/10.1007/s10533-025-01237-4.

E. Asmala (✉)
Environmental Geochemistry, Geological Survey of Finland, Espoo, Finland
e-mail: eero.asmala@gtk.fi

R. W. Paerl · C. L. Osburn
Department of Marine, Earth and Atmospheric Sciences, North Carolina State University, Raleigh, NC, USA
e-mail: rpaerl@ncsu.edu

C. L. Osburn
e-mail: closburn@ncsu.edu

Introduction

Estuaries act as coastal filters where biogeochemical processes modulate carbon (C) fluxes from terrestrial to marine ecosystems (Carstensen et al. 2020). Recent decades have seen increases in terrestrial organic carbon (OC) loading globally (Filella and Rodríguez-Murillo 2014; Asmala et al. 2019, 2021a). Flocculation, occurring at freshwater-seawater interfaces, involves seawater cations neutralizing the negative surface charge on dissolved organic matter (DOM; a complex mixture of organic substances that are small enough to pass through a filter, typically <0.2–0.7

Published online: 05 May 2025

μm) molecules, allowing DOM to aggregate into potentially sinking particles, ultimately being buried in coastal sediments (Ho et al. 2022). Flocculation is a key process in regulating OC sedimentation and subsequent burial and is thus significant for carbon cycling. However, its quantification is challenging due to the overlapping gradients in coastal systems and a variety of methodological approaches complicating cross-system comparisons.

Traditionally, flocculation has been studied by measuring suspended particulate matter (SPM) accumulation and the loss of dissolved constituents like dissolved organic carbon (DOC), providing insights into flocculation rates (Mikes et al. 2004; Khoo et al. 2022). Additionally, changes in optical characteristics such as chromophoric dissolved organic matter (CDOM) absorbance and fluorescence help understand the qualitative transformations (Asmala et al. 2014; Zhao et al. 2024). CDOM is the light-absorbing fraction of DOM, which affects water color and participates in key photochemical and biogeochemical processes. These varied methods highlight the challenge of precisely parameterizing flocculation-driven carbon transformations globally (Ward et al. 2020; Powley et al. 2024).

A unified methodological approach is crucial to improve estimates of terrestrial OC fate, influencing the distribution and deposition of OC and affecting coastal carbon sequestration (Bianchi and Allison 2009; Van de Broek et al. 2018). Variability in flocculation efficiency, i.e. removal of terrestrial DOC loading by flocculation is estimated to range from < 1 to 22%, which complicates understanding of land-to-sea carbon fluxes (Gustafsson et al. 2014; Clark et al. 2022; Powley et al. 2024). CDOM, a key variable in remote sensing applications, is used to trace terrestrial matter and correct data for chlorophyll, turbidity, and salinity (Fichot and Benner 2012; Matthews 2011). Specifically, CDOM absorbance in the visible range can be measured from satellite or airborne sensors to indicate the presence of terrestrially derived DOM in coastal and estuarine waters. This information helps differentiate between signals from organic matter and those from phytoplankton pigments or suspended sediments, thereby improving the accuracy of remote estimates of water quality parameters such as chlorophyll concentration and water clarity. Despite CDOM representing only a fraction of the DOC pool (Asmala et al. 2012), it is a widely used proxy for organic carbon due to its tight relationship with DOC across different aquatic environments (Massicotte et al. 2017).

The overall objective of this study was to examine the effect of salt-induced flocculation on CDOM absorption and fluorescence in five rivers in the United States and one in Finland and across seasons, to identify potential similarities in CDOM responses to flocculation. For this purpose, we quantified the changes in spectral CDOM absorption and fluorescence excitation-emission matrices (EEMs) in river water-seawater mixing experiments. We aimed to increase the amount of information gained from CDOM analysis by formulating the *red shift ratio* (balance between shorter and longer wavelength fluorescence signals) as a framework to compare the flocculation potential among various DOM sources.

Material and methods

Sampling sites

Five subtropical rivers in southeastern United States were sampled in June 2019 and boreal river Karjaanjoki in southern Finland was sampled six times throughout an annual cycle in 2017–2018 (Fig. S1). The five rivers sampled in North Carolina, United States, were Harvey Creek (Tar River basin), Neuse River (Neuse River basin), New River (Cape Fear basin), Newport River (White Oak basin), and Tar River (Tar River basin). These rivers were selected to cover latitudinal differences, as the United States rivers are located on 35°N and Karjaanjoki river on 60°N. River discharge data for Karjaanjoki was continuously measured from a gauged station (Table S2).

Mixing experiments

We carried out flocculation experiments by mixing sample water from study rivers with artificial seawater into final salinity of 2, and comparing the changes in DOM characteristics to reference units without salt addition (see Fig. S2 for a schematic representation of the experiment). This salinity value has previously been reported to be an important threshold for the flocculation of organic matter along estuarine mixing gradients (Lisitsyn 1995; Asmala et al. 2022). To avoid particle interference by adding incompletely

dissolved salt, we first prepared a salt solution (salinity 35) by diluting synthetic sea salt (Aquarium System Instant Ocean; EAN 3443980257502; Table S1) in ultrapure water. This solution was filtered through pre-combusted glass fiber filters (GF/F—nominal mesh size 0.7 µm; Cytiva Whatman) to remove any non-dissolved salts. Artificial salt solution (60 ml) was then mixed with the river water (940 ml) to the final salinity of 2, and reference samples were treated with equal volumes of ultrapure water. Incubations were carried out in acid-washed glass bottles in the dark at room temperature for 24 h (Asmala et al. 2014). At the end of the incubation, experimental samples were gently filtered through pre-combusted, pre-weighed GF/F filters, and the filtrates were collected for analyses. Aliquots of the filtrate for CDOM were stored at 4 °C until absorbance and fluorescence measurements were made within 72 h from sampling. Aliquots of the filtrate for DOC analyses were taken for US samples, acidified with 85% H_3PO_4, and stored frozen at − 20 °C until measurement. DOC analysis was not successful for Finnish samples due to issues with the instrumentation.

Laboratory analyses

We quantified CDOM absorbance using either a Shimadzu 2401PC (Karjaanjoki River) or a Varian Cary 300UV (US rivers) spectrophotometer, each equipped with a 1 cm quartz cuvette and covering a spectral range from 200 to 800 nm at 1 nm intervals. For all samples, we used ultrapure water as blank. We calculated the Napierian absorption coefficient (α, m^{-1}) from measured absorbance (A) using the equation $\alpha = 2.303 \times A/l$, where l is the optical path length of the cuvette (m). The $S_{275–295}$ and $S_{350–400}$ values, representing non-linear slopes of absorbance spectra within the 275–295 nm and 350–400 nm ranges, were determined with the cdom package in R software (Massicotte 2016a; Fig. S3). Further, we calculated the E2:E3 ratio, i.e. the ratio of absorption coefficients at 250 and 365 nm. For the measurement of fluorescent DOM (FDOM), a Varian Cary Eclipse fluorometer (Agilent Technologies, Santa Clara, CA, USA) was used (excitation range 220–450 nm; emission range 300–600 nm). We displayed results as excitation-emission matrices (EEMs). The EEMs were processed using the package eemR in R software (Massicotte 2016b). Each EEM was adjusted by deducting an ultrapure water blank, and after calibration Rayleigh and Raman scattering bands were discarded. Vendor-supplied corrections for excitation lamp energy and emission detector response were applied to each EEM. Calibration of EEMs involved normalization to the Raman water scatter peak area (at an excitation wavelength 350 nm) from an ultrapure water sample analyzed during the same session, and corrections for inner filter effects were applied using absorbance spectra (Murphy et al. 2010). From these corrected EEMs, the humification index (HIX) (Zsolnay et al. 1999) and biological index (BIX) (Huguet et al. 2009) were determined. We also calculated a *red shift ratio* to assess the potential systematic changes in EEMs from shorter emission wavelengths to longer wavelengths; specifically, the emission between 300 and 350 nm was divided by emission between 360 and 500 nm, at excitation 250–350 nm. This wavelength range was selected based on consistent patterns observed across samples, where fluorescence tended to decrease at shorter emission wavelengths and increase at longer wavelengths after flocculation. To standardize fluorescence data across laboratories, EEMs were averaged into 10 nm × 10 nm bins, compensating for differing original matrix dimensions. The concentration of DOC (µmol L^{-1}) was measured on an OI Analytical 1030D Aurora TOC analyzer in wet oxidation mode (Osburn and St-Jean 2007). Samples were sparged with ultrapure argon gas for 20 min to ensure that all dissolved inorganic carbon was removed. Calibration of DOC concentrations was done with NIST-traceable caffeine standards (typical error < 3%). Stable carbon isotope values were corrected for reagent blanks and normalized to the Vienna Pee Dee Belemnite (VPDB) scale using IAEA standards of sucrose (− 10.8‰) and caffeine (− 27.77‰). $SUVA_{254}$ is defined as the UV absorbance at 254 nm in (m^{-1}) divided by the DOC concentration (in milligrams per liter).

Statistical analyses

CDOM absorption and fluorescence measurements were corrected for the dilution introduced by addition of ultrapure water (reference samples) and artificial saltwater (treatment samples). In order to separate the effect of salt addition on from other effects caused by the experimental manipulations (dilution,

mixing etc.) on CDOM characteristics, the changes in reference samples were subtracted from the treatment samples. Changes to CDOM absorption or fluorescence due to flocculation are expressed as Eq. 1, where $CDOM_{BLANK}$ and $CDOM_{ASW\ BLANK}$ represents the absorption or fluorescence of ultrapure water and artificial salt solution, and $CDOM_{REFERENCE}$ and $CDOM_{TREATMENT}$ absorption or fluorescence values after additions of ultrapure water or artificial saltwater, respectively.

$$CDOM_{FLOC} = \left(CDOM_{TREATMENT} - CDOM_{ASWBLANK}\right) - \left(CDOM_{REFERENCE} - CDOM_{BLANK}\right) \quad (1)$$

It should be noted that artificial saltwater contained some additional CDOM signal compared to ultrapure water, but its effect on the final absorption and fluorescence was negligible (0.27% at 250 nm and 0.93% at 450 nm, on average) due to low amount added (~ 5% of the final volume) and the relatively high CDOM signal in our river water samples. Finally, CDOM absorption and fluorescence in reference samples was subtracted from the treatment samples (with saltwater addition). With this approach, spontaneous particle formation, sorption of DOM to the glass fiber filters, and other processes not caused by salt addition did not influence the results presented. Also, in this study the proportion of CDOM changes occurring due to "true" flocculation (particle formation from DOM due salt) or due to changes in DOM molecular conformations cannot be estimated, thus all changes are collectively attributed to salt-induced flocculation.

A Wilcoxon signed-rank test was used to evaluate if the median of the differential CDOM spectrum (before and after salt-induced flocculation) significantly differed from 0 to across all wavelengths. Simple linear regression was used to examine relationships between optical proxies and environmental variables.

Results

We observed considerable differences in changes in spectral CDOM absorption among seasons and sites (Fig. 1). Original CDOM spectra are presented in Fig. S4. In general, the absolute changes were the largest in shorter wavelengths, while relative changes were largest in longer wavelengths. Most observed changes were negative, meaning loss of CDOM absorption due to flocculation. In the Karjaanjoki River, where seasonal variability was examined, the largest changes due to flocculation in CDOM absorption occurred in November ($-1.4\ m^{-1}$; − 23% at 450 nm). In July, the changes were the smallest ($0.09\ m^{-1}$; 3% at 450 nm). Spatial variability was studied in five rivers across four river basins in the Southeastern United States, and the decrease in absorption ranged from $-0.16\ m^{-1}$ (− 3%) in the New River to $-0.51\ m^{-1}$ (− 15%) in the Neuse River at 450 nm.

Changes in CDOM fluorescence varied largely among seasons and sites (Figs. 2 and 3). Original excitation-emission matrices in Raman units (R.U.) are presented in Fig. S5. As a general pattern, we observed decreased fluorescence intensity in the emission region below ca. 350 nm, which corresponds roughly to the protein-like peaks B and T (Coble 1996). Conversely, in the higher emission wavelengths (350–500 nm; including e.g. humic-like peak C), the fluorescence intensity was typically increasing due to flocculation. This pattern is also apparent in humification index (HIX), which increases in all but one occasion (Fig. S6). Changes in EEMs ranged between − 0.10 and 0.12 R.U., with the strongest decreases in Newport River and increases in Neuse River. Karjaanjoki River showed high temporal variability in both original fluorescence intensities and the absolute difference caused by flocculation. In Karjaanjoki samples, there was a decrease in the lower emission wavelength region (Ex 250–330 nm; Em < 350 nm) in all but one of the six sampling occasions, ranging from − 9.3 to − 1.9%. In August, we observed an increase of 3.5% in the fluorescence intensity in this region dominated by protein-like fluorescence. In the five United States rivers, the observed change in this lower emission wavelength region of EEMs ranged from −13.6% (Newport River) to 9.7% (Neuse River). The changes in the higher emission wavelengths (Ex > 250 nm; Em > 350 nm) ranged from − 1.0% (May) to 3.7% (August) in Karjaanjoki, whereas in United States rivers the observed changes were − 1.7% (Neuse River)—3.5% (New River).

Using the observed changes in individual CDOM absorption spectra and fluorescence EEMs (Figs. 1, 2 and 3), we summarized the universal change in CDOM properties due to flocculation (Fig. 4). Across all 11 samples from study sites, the relative change

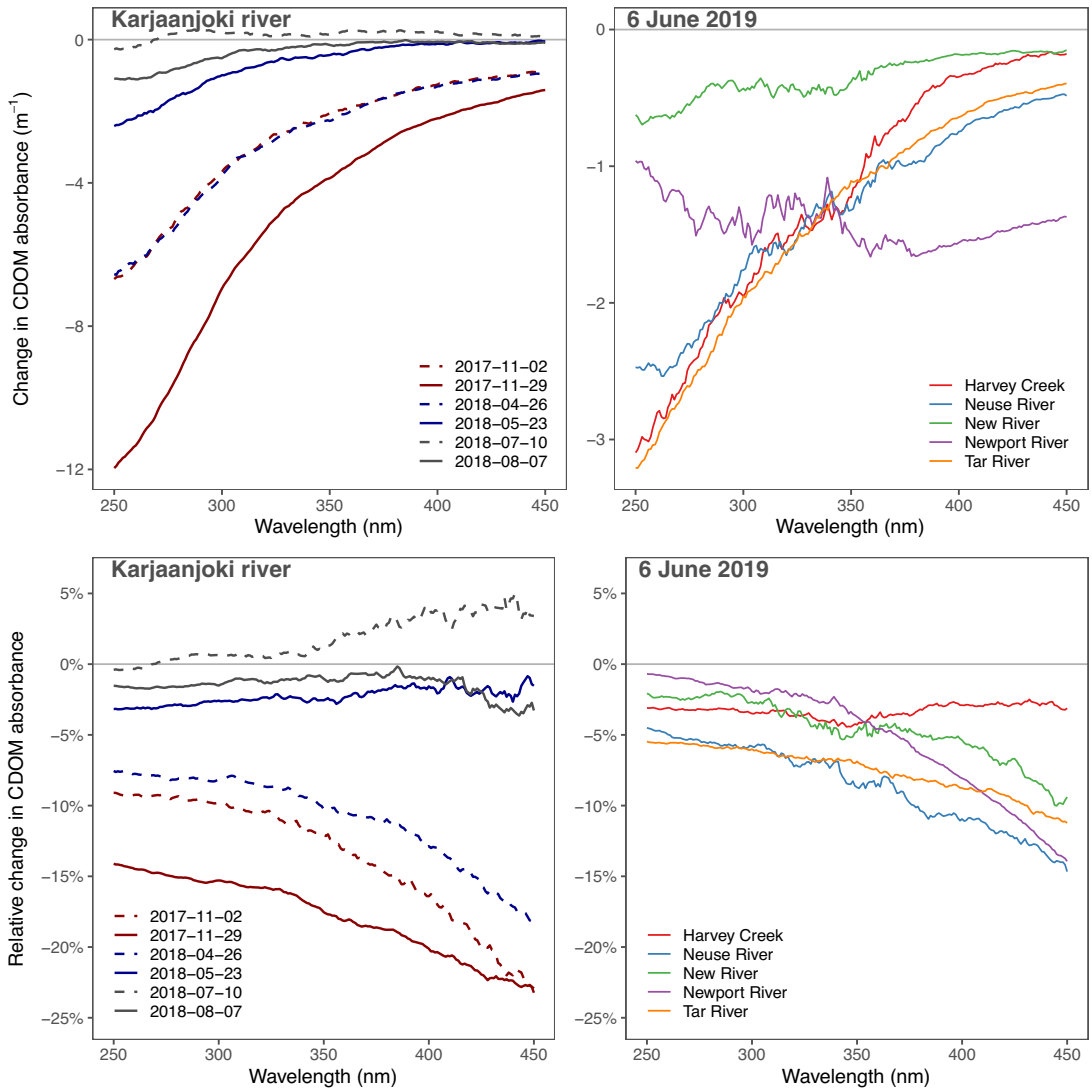

Fig. 1 Changes in spectral colored dissolved organic matter (CDOM) absorption in the wavelength range 250–450 nm (top row absolute values; bottom row relative values) due to flocculation at salinity 2. Temporal dynamics are presented from Karjaanjoki River (left column) and system-specific dynamics in five different river systems (right column). Positive relative values indicate net increase in CDOM absorption at a given wavelength, negative values indicate decrease in CDOM absorption

in CDOM absorption followed a negative exponential curve (Fig. 4a), where the rate of decrease in CDOM absorption signal increased with increasing wavelength. The CDOM absorption decrease was 4.7 ± 4.1% at 250 nm, and 10.8 ± 8.8% at 450 nm (mean ± 1SD). From the CDOM fluorescence, we identified a breakpoint between emission wavelengths 360 and 370 nm, where change in fluorescence intensity shifted from negative to positive (Fig. 3b). The largest decrease (− 11.7%) was observed at ex/em 250/300 nm, and the largest increase at ex/em 390/460 nm.

The E2:E3 ratio (ratio between A_{250} and A_{365}) ranged from 4.27 to 6.45, varying across seasons and locations (Fig. 5). The changes in E2:E3 were mostly positive, meaning that the ratios increased due to flocculation, ranging from − 0.17 to 0.28. On the other hand, the red shift ratio ($Em_{300–350}$:$Em_{360–500}$ at $Ex_{250–300}$) showed consistent decrease (Fig. 4).

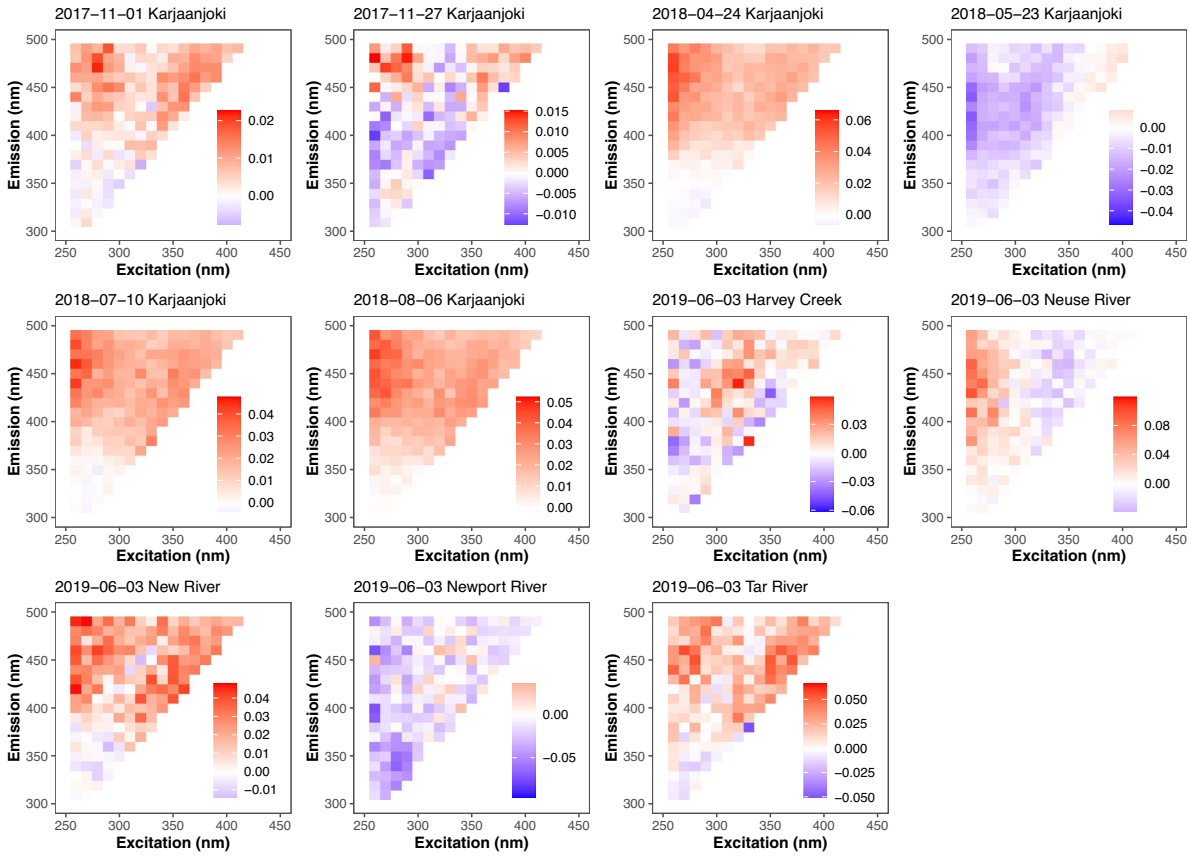

Fig. 2 Changes in colored dissolved organic matter (CDOM) fluorescence excitation-emission matrices (in Raman units) due to flocculation at salinity 2. Changes are expressed as Raman units. Temporal dynamics are presented from Karjaanjoki River and system-specific dynamics in five different river systems. Positive values (red) indicate an increase in CDOM fluorescence at a given excitation-emission wavelength, negative values (blue) indicate decrease in CDOM fluorescence excitation-emission

The red shift ratio values ranged between 0.0161 and 0.0277, and the change values between − 0.0036 and 0.0002.

Exploring the linkages between flocculation sensitivity and environmental drivers showed that change in E2:E3 (ΔE2:E3) due to flocculation was tightly coupled to river discharge (Fig. 6a). The relationship was direct, meaning that the changes in E2:E3 increased with increasing discharge values. Change in red shift ratio ($\Delta Em_{300–350}$:$Em_{360–500}$) showed no significant relationship with discharge (Fig. 6b). Initial DOM characteristics, as indicated by DOC-specific UV absorbance ($SUVA_{254}$) and stable carbon isotope signature of DOC (δ^{13}C-DOC), were also linked with changes in ratios (data shown in Table S3). $SUVA_{254}$ had a positive relationship with ΔE2:E3, and δ^{13}C-DOC showed a positive relationship with $\Delta Em_{300–350}$:$Em_{360–500}$.

Discussion

Spatio-temporal variability in CDOM changes

We observed decreases throughout the CDOM absorption spectrum due to salt-induced flocculation, and also notable changes in the CDOM fluorescence EEMs (Figs. 1 and 2). Compared to CDOM absorption, which showed more uniform relative decreases across systems, FDOM responses appeared more site-specific, likely reflecting localized differences in DOM composition, sources,

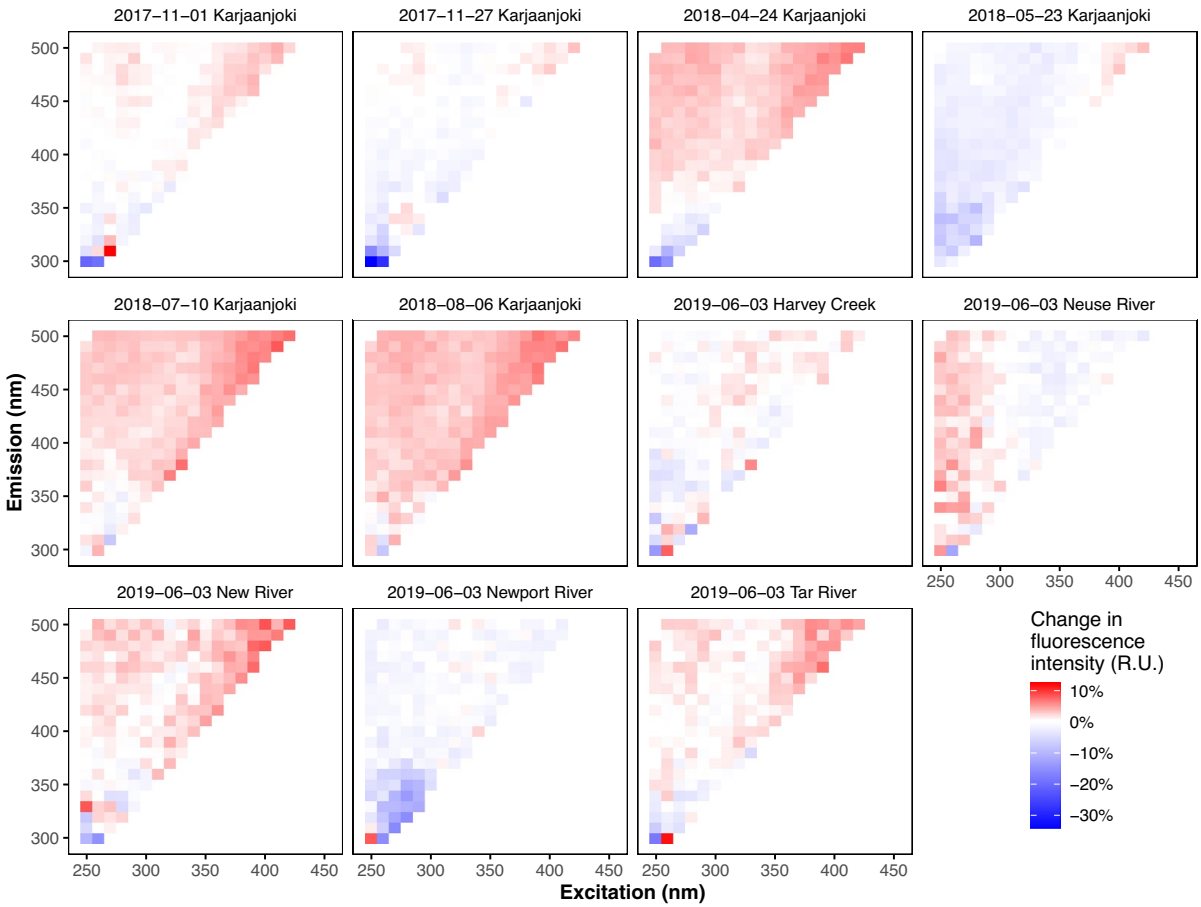

Fig. 3 Relative changes in colored dissolved organic matter (CDOM) fluorescence excitation-emission matrices due to flocculation at salinity 2. Changes are expressed as relative values, normalized to the original values of the river water EEMs, to quantify the effects of the salt treatment independently of the initial intensities. Temporal dynamics are presented from Karjaanjoki River and system-specific dynamics in five different river systems. Positive relative values (red) indicate net increase in CDOM fluorescence at a given excitation-emission wavelength, negative values (blue) indicate decrease in CDOM fluorescence excitation-emission

and biogeochemical processing prior to mixing. Our observations concur with previous experimental findings, where consistent changes along the UV–Vis absorption spectrum and fluorescence EEMs have been observed (Asmala et al. 2014; Virtasalo et al. 2023). Spectral CDOM absorption in samples from Finland decreased more during spring and autumn, periods characterized by cooler temperatures and higher river discharge, compared to the smaller changes observed in summer. This seasonality was mirrored in the changes in EEMs, with notable decreases in spring and autumn and smaller decreases coupled with larger increases in summer. These seasonal differences can be attributed to the origin and reactivity of DOM, which changes seasonally due to altering hydrological conditions (Stedmon et al. 2006; Spencer et al. 2008; Fellman et al. 2009). During the high flow regime, fresher, more labile humic DOM is introduced into subtropical river networks from adjacent wetlands, which is reflected in our samples from the United States (Rudolph et al. 2020). On the other hand, and in particular for boreal rivers, low precipitation conditions result in the transport of older, more humified DOM through groundwater pathways, characterized by higher aromaticity and a greater proportion of less bioavailable humic substances (Singh et al. 2014; Fasching et al. 2016). Spatially, despite

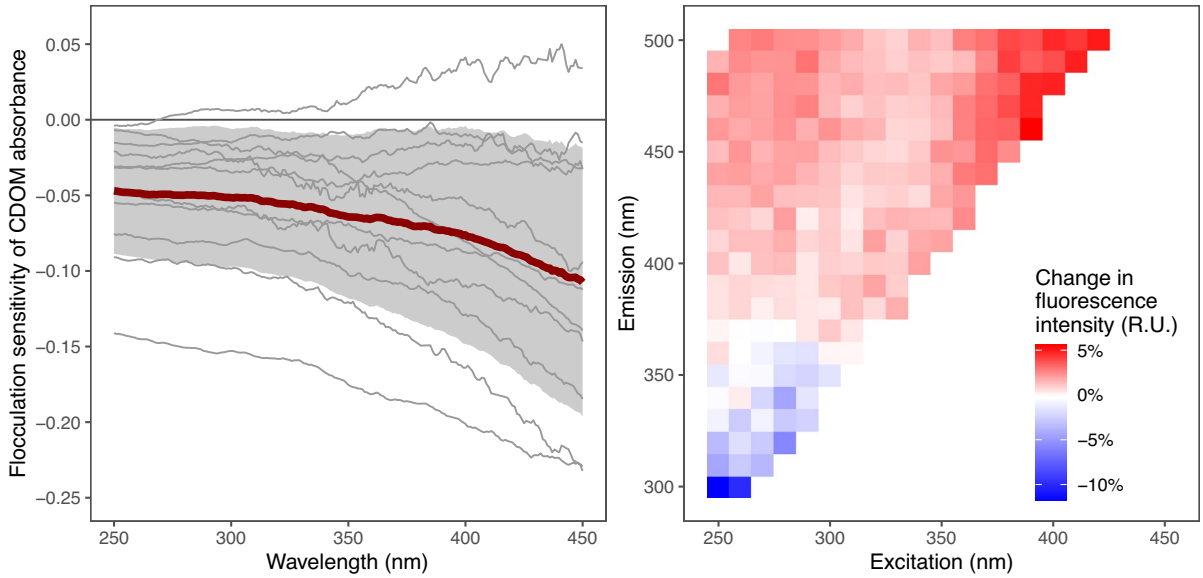

Fig. 4 Average relative changes in colored dissolved organic matter (CDOM) optical properties across sampling campaigns due to flocculation at salinity 2 (n = 11). In panel a), thick red line indicates the average change in CDOM absorption in the wavelength range 250–450 nm range, gray shaded area indicates ±1SD, and the 11 individual sampling campaigns are shown as thin gray lines. Resulting average change is significantly different from 0 ($p < 0.001$). In panel b), the average change in CDOM fluorescence in the excitation-emission matrix

initially considerable differences in spectral CDOM absorption and EEMs across study locations, the changes post-flocculation were surprisingly uniform (Fig. 1). The temporal control of changes in CDOM is clear also in the tight coupling of ΔE2:E3 with discharge (Fig. 6a). Our results suggest that seasonal and temporal variations in biogeochemical processes, such as changes in hydrological pathways (including catchment characteristics), microbial activities, and sunlight exposure, are a major factor influencing the sensitivity of DOM to salt-induced flocculation. These processes affect both the concentration and the composition of DOM by altering its molecular structure, aromaticity, and reactivity. In particular, the origin and processing history of DOM, shaped by upstream biological and photochemical transformations, may determine how readily it flocculates upon mixing with saltwater. These effects act in combination with the inherent chemical properties of DOM, such as molecular weight and functional group composition, to shape its flocculation response (Fig. 6c–f). While the intrinsic characteristics of DOM do vary with the seasons, these fluctuations are potentially overshadowed by the more pronounced effects of environmental factors described above in shaping DOM responses.

Mechanisms behind observed changes in CDOM absorption and fluorescence

The decrease in CDOM absorption was not uniform throughout the measured spectrum (250–450 nm), but the decrease was more pronounced within the visible wavelength range compared to the UV range (Figs. 1 and 4a). CDOM absorption increased on only one occasion (July sampling) due to flocculation, suggesting that under low river discharge conditions, salt-induced molecular rearrangement (charge screening and structural reorganization) likely exposed previously quenched chromophores, thus enhancing UV–Vis absorption (Cuss and Guéguen 2015; Stedmon and Markager 2001). The non-linear change across the absorption spectrum is very pronounced in the changes in E2:E3 ratio, showing systematic increases due to flocculation (Fig. 5). This change suggests a preferential removal of high-molecular-weight, aromatic DOM, leaving behind a relatively greater proportion of (originally)

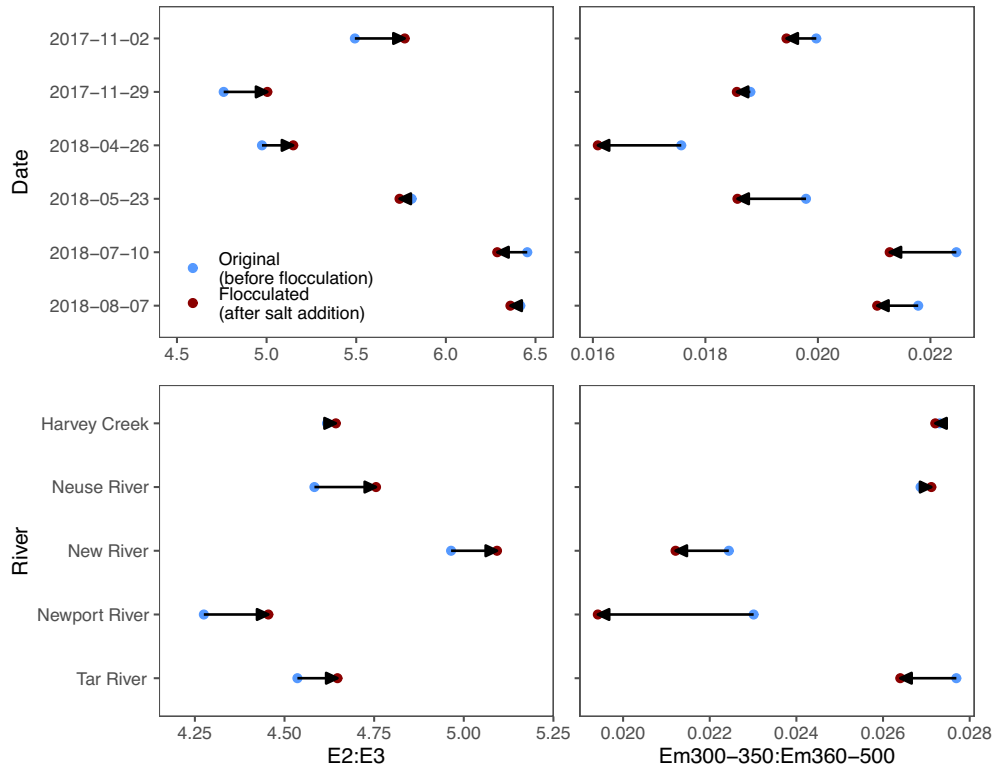

Fig. 5 Changes in optical ratios used to assess DOM transformation due to flocculation. Left column shows the change in E2:E3 ratio (absorption at 250 nm divided by absorption at 365 nm). Right column shows the change in red shift ratio (Em300-350:Em360-500; Ex250-300). Positive values indicate increases in the respective ratios following salt-induced flocculation

low-molecular-weight DOM (Santos et al. 2016; Aulló-Maestro et al. 2017). This pattern is consistent with the concept of flocculation-driven fractionation, where larger, more aromatic molecules aggregate and are removed, while smaller, less condensed structures remain in solution, shifting the DOM pool toward a higher E2:E3 ratio.

Fluorescence responses also varied, but in most cases we observed an increase in absolute fluorescence values at higher emission wavelengths, and a decrease in shorter emission wavelengths (Fig. 2). In few cases, we observed a decreasing fluorescence at higher emission wavelengths (Fig. 2), and these occurred when protein-like fluorescence was the lowest. This suggests that flocculation was particularly efficient at removing not only freshly produced, microbial DOM (Peak T) but also a fraction of humic-like, high-molecular-weight DOM during these occasions. Overall, we observed a systematic decrease in emission at 300–350 nm and an increase at 360–500 nm (excitation wavelength 250–300 nm) (Figs. 2 and 4b). This change is well represented by the red shift ratio ($Em_{300–350}$:$Em_{360–500}$), which decreased in all but one experimental unit (Fig. 5). The observed increase in E2:E3 (A_{250}/A_{365}) and simultaneous decrease in the red shift ratio due to salt-induced flocculation suggests a selective transformation in DOM composition rather than uniform removal.

The preferential flocculation of low-molecular-weight, protein-like DOM led to a greater loss of fluorescence at Em 300–350 nm, while charge screening and molecular restructuring increased fluorescence efficiency at Em 360–500 nm. Also, the decrease in spectral CDOM absorption and fluorescence intensities at <350 nm implies a transformation of smaller, aromatic terrestrial-derived compounds into larger aggregates (Baalousha et al. 2006; Asmala et al. 2021b), while the increase in

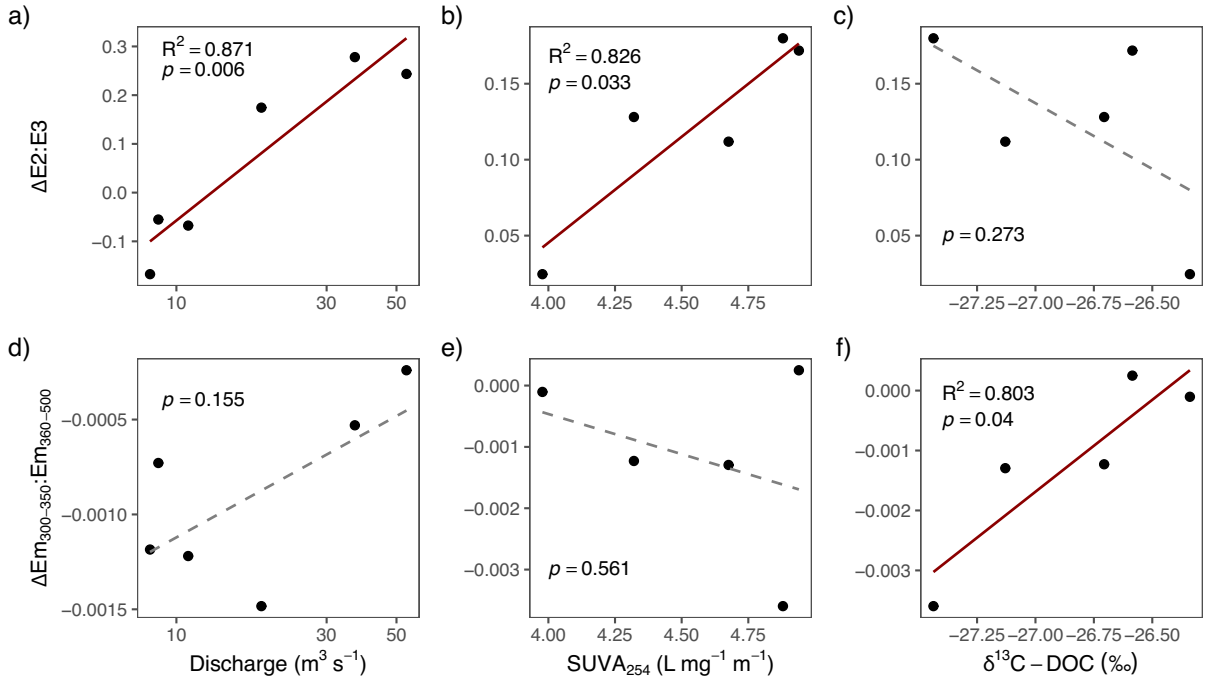

Fig. 6 Relationships between river discharge (**a**, **d**), initial DOC-specific UV absorbance ($SUVA_{254}$) (**b**, **e**) and stable carbon isotope signature of DOC (δ^{13}C-DOC) (**c**, **f**), and changes in E2:E3 (top row) and $Em_{300-350}$:$Em_{360-500}$ (bottom row). The relationship with discharge was assessed only for the temporally-resolved sampling in Karjaanjoki river (n = 6), and the relationship with initial DOM variables only for the spatially-resolved dataset (n = 5). Significant linear relationships ($p < 0.05$) are marked with solid red line and adjusted R-squared value is given. Gray dashed line indicates non-significant linear relationship

fluorescence at higher wavelengths indicates the relative enrichment or formation of larger, more complex molecules (Cuss and Guéguen 2015). Further, humification index (HIX), which compares two broad aromatic-dominated fluorescence maxima at emission wavelengths 435–480 nm and 300–345 nm, increased in general, implying an increase in the carbon-to-hydrogen ratio and with a resulting shift to longer emission wavelength (Zsolnay et al. 1999). These findings further support the molecular alterations and aggregation processes due to salt-induced flocculation, leading to changes in the chemical structure or aggregation state of organic matter (Souza Sierra et al. 1997; Ho et al. 2022). These alterations highlight the nuanced interplay between conformational changes, quenching effects and the formation of new complexes due to salt-induced flocculation, collectively contributing to the observed red shift in CDOM fluorescence (Esteves et al. 1999; Romera-Castillo et al. 2014).

The linkages between the observed increase in E2:E3 (ΔE2:E3) and $SUVA_{254}$ values, along with the decrease in the red shift ratio and δ^{13}C-DOC signature (Fig. 6), suggest a structured transformation in DOM composition during salt-induced flocculation (Fig. 7). The preferential removal of low-molecular-weight, aliphatic-rich DOM (A_{250}-associated CDOM) led to an enrichment of high-molecular-weight, aromatic compounds, resulting in higher $SUVA_{254}$ and E2:E3 values, consistent with previous findings that flocculation selectively removes less aromatic DOM while leaving behind more humic-rich material (Asmala et al. 2014; Stedmon and Markager 2001). Simultaneously, the stronger decrease in protein-like fluorescence (Em 300–350 nm) relative to humic-like fluorescence (Em 360–500 nm) contributed to a declining red shift ratio, while the associated removal of microbially processed, ^{13}C-enriched DOM led to a shift in δ^{13}C-DOC toward more negative values, reflecting a greater relative contribution of terrestrial-derived, lignin-rich DOC (Raymond and

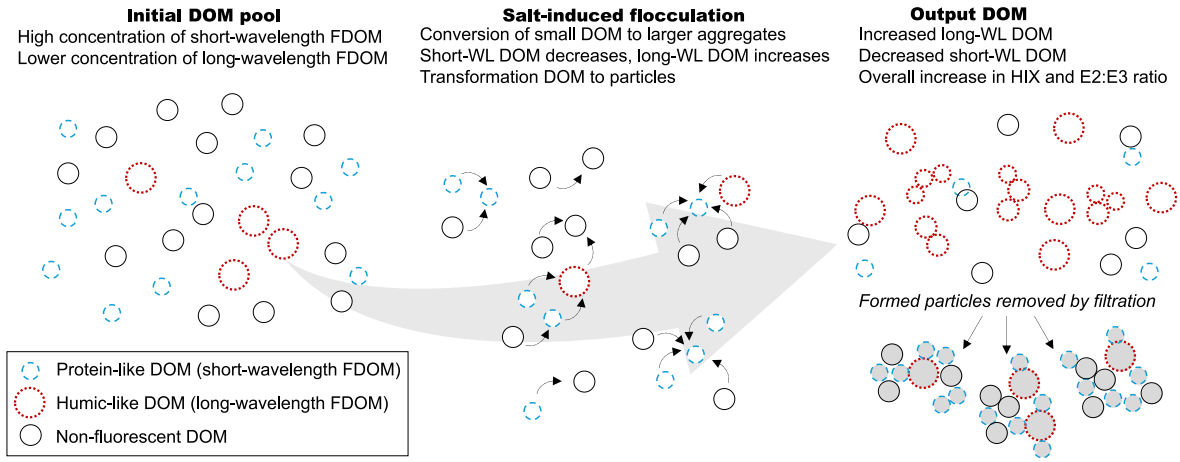

Fig. 7 Schematic illustration of dissolved organic matter (DOM) transformation during salt-induced flocculation. The initial DOM pool (left) has relatively higher proportion of protein-like, low molecular weight DOM (short-wavelength fluorescent DOM; FDOM), with a smaller fraction of humic-like, high molecular weight DOM (long-wavelength FDOM). During the flocculation process (center), salt-induced aggregation leads to the conversion of small-size DOM to larger aggregates and formation of particles, accompanied by a red shift in DOM fluorescence. As a result, the transformed DOM pool (right) exhibits an increased proportion of humic-like DOM and decreased protein-like DOM. This transformation leads to an increase in humification index (HIX) and E2:E3 ratio, reflecting the preferential removal of protein-like, freshly produced DOM and relative enrichment of aromatic, humic-like compounds

Bauer 2001; Fellman et al. 2010). These patterns suggest that flocculation not only acts as a removal process for riverine CDOM but also alters its optical and isotopic characteristics in a way that favors the retention of more aromatic and terrestrial-like components in the dissolved phase. This restructuring of the DOM pool during estuarine mixing has important implications for DOM bioavailability, microbial utilization, and carbon sequestration in coastal waters.

Optical changes and conservative mixing

In estuarine systems, freshwater and seawater interactions are often modeled using conservative mixing assumptions, where the concentration of dissolved substances changes linearly along a salinity gradient (Liss 1976). However, non-conservative processes such as flocculation disrupt this assumption by altering the transport, deposition, and transformation of DOM and particulates (Uher et al. 2001; Jilbert et al. 2018). A simplified representation of these two scenarios is presented in Fig. 8, showing how flocculation leads to deviations from the conservative mixing line. When optical measurements are employed to infer terrestrial DOC loading or biogeochemical processes within the estuarine salinity gradient, assuming conservative mixing can introduce systematic errors by neglecting flocculation as a removal term for DOC. These findings suggest that integrating optical parameters, such as E2:E3 and fluorescence red shift, into estuarine models could improve the accuracy of DOM flux estimates.

By parameterizing optical flocculation proxies (such as red shift ratio), models could simulate the variable efficiency of OC removal through flocculation under different environmental conditions (e.g., salinity, DOC composition, turbulence). The parameterization could involve for example: (1) empirical relationships between flocculation "efficiency" and environmental variables (e.g., salinity, SPM concentration) (Ho et al. 2022), (2) empirical relationships between flocculation and source OC characteristics (chemical composition, catchment land-use, elemental stoichiometry etc.) (Khoo et al. 2022), (3) process-based models that simulate the kinetics of floc formation and sedimentation based on optical data (Maerz et al. 2011), and (4) spatial variability of optical proxies across different estuarine

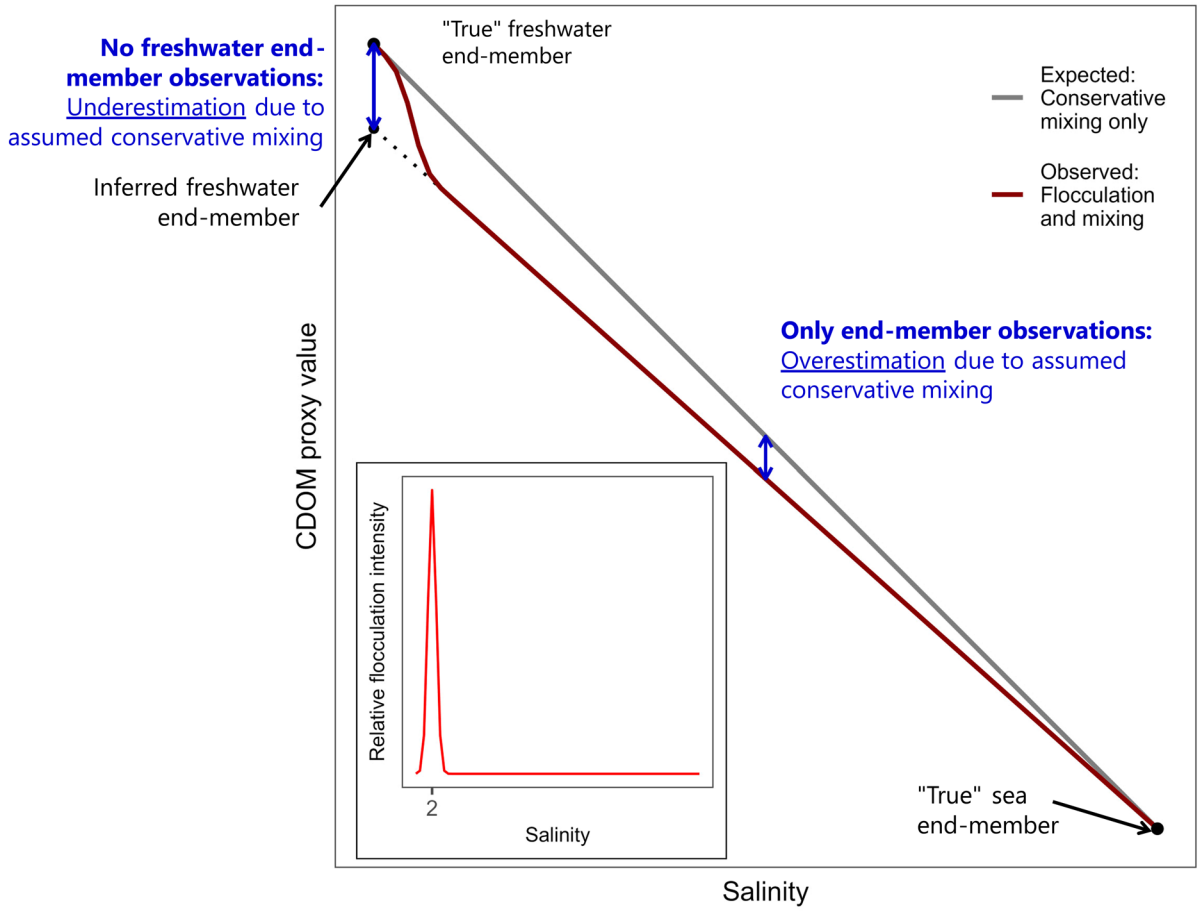

Fig. 8 Schematic overview of the effect of flocculation on assumed conservative mixing along an estuarine salinity gradient. The main panel shows the concentration of a proxy value (e.g. $a_{CDOM(254)}$) on two mixing lines along a salinity gradient: (1) conservative mixing line between two end-members (gray line), and (2) non-conservative mixing line between two end-members, affected by flocculation (red line). Flocculation is assumed to peak at salinity 2 (inset figure) and be negligible at other salinities

systems to capture the heterogeneity in flocculation processes globally.

Implications for carbon biogeochemistry

Our observations suggest a common response in spectral CDOM absorption and fluorescence EEMs to salt-induced flocculation across both boreal and subtropical coastal rivers. This implies ubiquity of the process and warrants further investigation in other coastal regions. Use of optical proxies is justified to confirm the universality of flocculation as a mechanism for the aggregation and subsequent removal by sedimentation of organic carbon across coastal rivers, over seasons, and in response to climate change. We revealed a 5–10% decrease in CDOM absorption due to flocculation, indicative of removal of colored dissolved compounds via particle formation. Using this information, we can estimate the flocculation sink term for riverine DOC in by using the observed reduction of 4.8% in CDOM absorption at 254 nm due to flocculation. At this wavelength, the colored fraction of the total DOC pool has a lower bound of 41% and an upper bound of 82% (Asmala et al. 2012). Assuming that flocculation affects only this colored fraction, we applied the CDOM loss specifically to this portion of the DOC pool. We then considered global estimates of riverine DOC inputs

to the coastal ocean, ranging from 238 Tg yr^{-1} (Li et al. 2017) to 420 Tg yr^{-1} (Battin et al. 2023). As a result, we estimate that the potential flocculation sink term for terrestrial DOC ranges from 4.7 Tg yr^{-1} to 16.7 Tg yr^{-1}. This estimated sink term corresponds to 1.9% to 6.6% of the annual carbon sink in the global coastal ocean, including estuaries (Dai et al. 2022). It should be noted that this estimate is based on findings from the limited number of locations used in this study, increasing its uncertainty in the global context. However, to quantitatively estimate terrestrial organic carbon sedimentation resulting from flocculation, future studies need data on geochemical markers that trace freshly formed flocs from surface waters to sediments in estuaries, and specific biomarkers to identify the sources of organic carbon.

Better spatial coverage of optical flocculation indices would improve our understanding about the variability of flocculation across different systems and help identify regions where terrestrial OC is more likely to be flocculated and potentially creating sedimentary carbon burial hot spots (Bianchi et al. 2018). These together would refine models of carbon cycling and storage at regional and global scales. Correspondingly, this has significant implications for the use of CDOM as a conservative tracer of terrestrial DOC and for remote sensing of DOC in coastal and estuarine waters. Notably, the absorption loss was most pronounced in the visible wavelength range, critical for remote sensing applications (Brezonik et al. 2015), and was closely associated with discharge levels, highlighting the role of hydrological variability in carbon fluxes along the land-sea continuum, considering climate-influenced weather drivers of that variability (e.g., Osburn et al. 2019). These findings caution the applicability of CDOM as a conservative tracer along the land-sea continuum, suggesting adjustments in remote sensing algorithms and estimations of carbon mass fluxes in coastal and estuarine environments may be necessary.

The observed optical changes have broader implications for carbon cycling in estuaries and coastal environments. The shift from high molecular weight, humic-rich DOM to more low molecular weight, microbially available DOM has implications for microbial carbon processing and burial efficiency. Flocculation-induced removal of CDOM represents a mechanism by which terrestrially derived organic carbon is sequestered in estuarine sediments rather than transported to the open ocean. This process likely varies seasonally and spatially, influencing the efficiency of estuarine carbon burial. Given the sensitivity of E2:E3 and fluorescence red shift to salinity-driven DOM transformations, these optical ratios may serve as valuable proxies for quantifying flocculation effects in future studies. Further research should focus on integrating optical metrics with geochemical markers to trace flocculation-derived sedimentary carbon pools across different estuarine environments.

Acknowledgements We would like to extend our gratitude to Dr. Urban Wünsch for useful discussions about sensitivity of DOM to various biogeochemical processes. We would like to thank the staff and interns from Tvärminne Zoological Station for support in field sampling and laboratory activities. EA was supported by the Academy of Finland (Grant No. 309748).

Author contributions EA designed and conducted the Karjaanjoki field campaigns and experiments. All authors designed and carried out field campaigns and experiments in the United States. CO supported the laboratory analyses. EA did the formal analyses and wrote the first draft of the manuscript. All authors contributed to writing the manuscript and approved the submitted version.

Funding Open Access funding provided by Geological Survey of Finland. EA was supported by the Academy of Finland (Grant No. 309748).

Data availability Data will be made available at PANGAEA data repository (www.pangaea.org).

Declarations

Competing interests The authors have not disclosed any competing interests.

Open Access This article is licensed under a Creative Commons Attribution 4.0 International License, which permits use, sharing, adaptation, distribution and reproduction in any medium or format, as long as you give appropriate credit to the original author(s) and the source, provide a link to the Creative Commons licence, and indicate if changes were made. The images or other third party material in this article are included in the article's Creative Commons licence, unless indicated otherwise in a credit line to the material. If material is not included in the article's Creative Commons licence and your intended use is not permitted by statutory regulation or exceeds the permitted use, you will need to obtain permission directly from the copyright holder. To view a copy of this licence, visit http://creativecommons.org/licenses/by/4.0/.

References

Asmala E, Stedmon CA, Thomas DN (2012) Linking CDOM spectral absorption to dissolved organic carbon concentrations and loadings in boreal estuaries. Estuar Coast Shelf Sci 111:107–117

Asmala E, Bowers DG, Autio R, Kaartokallio H, Thomas DN (2014) Qualitative changes of riverine dissolved organic matter at low salinities due to flocculation. J Geophys Res Biogeosci 119:1919–1933

Asmala E, Carstensen J, Räike A (2019) Multiple anthropogenic drivers behind upward trends in organic carbon concentrations in boreal rivers. Environ Res Lett 14:124018

Asmala E, Osburn CL, Paerl RW, Paerl HW (2021a) Elevated organic carbon pulses persist in estuarine environment after major storm events. Limnol Oceanogr Lett 6:43–50

Asmala E, Massicotte P, Carstensen J (2021b) Identification of dissolved organic matter size components in freshwater and marine environments. Limnol Oceanogr 66:1381–1393

Asmala E, Virtasalo JJ, Scheinin M, Newton S, Jilbert T (2022) Role of particle dynamics in processing of terrestrial nitrogen and phosphorus in the estuarine mixing zone. Limnol Oceanogr 67:1–12

Aulló-Maestro ME, Hunter P, Spyrakos E, Mercatoris P, Kovács A, Horváth H, Tyler A (2017) Spatio-seasonal variability of chromophoric dissolved organic matter absorption and responses to photobleaching in a large shallow temperate lake. Biogeosciences 14(5):1215–1233

Baalousha M, Motelica-Heino M, Le Coustumer P (2006) Conformation and size of humic substances: effects of major cation concentration and type, pH, salinity, and residence time. Coll Surf A Physicochem Eng Asp 272:48–55

Battin TJ, Lauerwald R, Bernhardt ES, Bertuzzo E, Gener LG, Hall RO Jr, Regnier P (2023) River ecosystem metabolism and carbon biogeochemistry in a changing world. Nature 613:449–459

Bianchi TS, Allison MA (2009) Large-river delta-front estuaries as natural "recorders" of global environmental change. Proc Natl Acad Sci USA 106:8085–8092

Bianchi TS, Cui X, Blair NE, Burdige DJ, Eglinton TI, Galy V (2018) Centers of organic carbon burial and oxidation at the land-ocean interface. Org Geochem 115:138–155

Brezonik PL, Olmanson LG, Finlay JC, Bauer ME (2015) Factors affecting the measurement of CDOM by remote sensing of optically complex inland waters. Remote Sens Environ 157:199–215

Carstensen J, Conley DJ, Almroth-Rosell E, Asmala E, Bonsdorff E, Fleming-Lehtinen V, Zilius M (2020) Factors regulating the coastal nutrient filter in the Baltic Sea. Ambio 49:1194–1210

Clark JB, Mannino A, Tzortziou M, Spencer RG, Hernes PJ (2022) The transformation and export of organic carbon across an arctic river-delta-ocean continuum. J Geophys Res Biogeosci 127:e2022JG007139

Coble PG (1996) Characterization of marine and terrestrial DOM in seawater using excitation-emission matrix spectroscopy. Mar Chem 51:325–346

Cuss CW, Guéguen C (2015) Relationships between molecular weight and fluorescence properties for size-fractionated dissolved organic matter from fresh and aged sources. Water Res 68:487–497

Dai M, Su J, Zhao Y, Hofmann EE, Cao Z, Cai WJ, Wang Z (2022) Carbon fluxes in the coastal ocean: synthesis, boundary processes, and future trends. Annu Rev Earth Planet Sci 50:593–626

de Souza Sierra MM, Donard OF, Lamotte M (1997) Spectral identification and behaviour of dissolved organic fluorescent material during estuarine mixing processes. Mar Chem 58:51–58

Esteves V, Santos EH, Duarte A (1999) Study of the effect of pH, salinity and DOC on fluorescence of synthetic mixtures of freshwater and marine salts. J Environ Monit 1:251–254

Fasching C, Ulseth AJ, Schelker J, Steniczka G, Battin TJ (2016) Hydrology controls dissolved organic matter export and composition in an Alpine stream and its hyporheic zone. Limnol Oceanogr 61:558–571

Fellman JB, Hood E, D'Amore DV, Edwards RT, White D (2009) Seasonal changes in the chemical quality and biodegradability of dissolved organic matter exported from soils to streams in coastal temperate rainforest watersheds. Biogeochemistry 95:277–293

Fellman JB, Hood E, Spencer RG (2010) Fluorescence spectroscopy opens new windows into dissolvedorganic matter dynamics in freshwater ecosystems: A review. Limnology and oceanography 55(6):2452–2462

Fichot CG, Benner R (2012) The spectral slope coefficient of chromophoric dissolved organic matter (S275–295) as a tracer of terrigenous dissolved organic carbon in river-influenced ocean margins. Limnol Oceanogr 57:1453–1466

Filella M, Rodríguez-Murillo JC (2014) Long-term trends of organic carbon concentrations in freshwaters: strengths and weaknesses of existing evidence. Water 6:1360–1418

Gustafsson E, Deutsch B, Gustafsson BG, Humborg C, Mörth CM (2014) Carbon cycling in the Baltic Sea—The fate of allochthonous organic carbon and its impact on air–sea CO2 exchange. J Mar Syst 129:289–302

Ho QN, Fettweis M, Spencer KL, Lee BJ (2022) Flocculation with heterogeneous composition in water environments: a review. Water Res 213:118147

Huguet A, Vacher L, Relexans S, Saubusse S, Froidefond JM, Parlanti E (2009) Properties of fluorescent dissolved organic matter in the Gironde Estuary. Org Geochem 40:706–719

Jilbert T, Asmala E, Schröder C, Tiihonen R, Myllykangas JP, Virtasalo JJ, Hietanen S (2018) Impacts of flocculation on the distribution and diagenesis of iron in boreal estuarine sediments. Biogeosciences 15:1243–1271

Khoo CL, Sipler RE, Fudge AR, Beheshti Foroutani M, Boyd SG, Ziegler SE (2022) Salt-induced flocculation of dissolved organic matter and iron is controlled by their concentration and ratio in boreal coastal systems. J Geophys Res Biogeosci 127:e2022JG006844

Li M, Peng C, Wang M, Xue W, Zhang K, Wang K, Zhu Q (2017) The carbon flux of global rivers: a re-evaluation of amount and spatial patterns. Ecol Indic 80:40–51

Lisitsyn AP (1995) The marginal filter of the ocean. Oceanology 34:671–682

Liss PS (1976) Conservative and non-conservative behavior of dissolved constituents during estuarine mixing. In: Estuarine chemistry. Academic Press, London, pp 93–130

Maerz J, Verney R, Wirtz K, Feudel U (2011) Modeling flocculation processes: Intercomparison of a size class-based model and a distribution-based model. Cont Shelf Res 31:S84–S93

Massicotte P, Asmala E, Stedmon C, Markager S (2017) Global distribution of dissolved organic matter along the aquatic continuum: across rivers, lakes and oceans. Sci Total Environ 609:180–191

Massicotte P (2016a) cdom: Wrapper functions to model and extract various quantitative information from absorption spectra of chromophoric dissolved organic matter (CDOM), CRAN [code]. https://CRAN.R-project.org/package=cdom

Massicotte P (2016b) eemR: tools for pre-processing emission-excitation matrix (EEM) fluorescence data, CRAN [code]. https://CRAN.R-project.org/package=eemR

Matthews MW (2011) A current review of empirical procedures of remote sensing in inland and near-coastal transitional waters. Int J Remote Sens 32:6855–6899

Mikes D, Verney R, Lafite R, Belorgey M (2004) Controlling factors in estuarine flocculation processes: experimental results with material from the Seine Estuary, Northwestern France. J Coast Res 41:82–89

Murphy KR, Butler KD, Spencer RG, Stedmon CA, Boehme JR, Aiken GR (2010) Measurement of dissolved organic matter fluorescence in aquatic environments: an interlaboratory comparison. Environ Sci Technol 44:9405–9412

Osburn CL, St-Jean G (2007) The use of wet chemical oxidation with high-amplification isotope ratio mass spectrometry (WCO-IRMS) to measure stable isotope values of dissolved organic carbon in seawater. Limnol Oceanogr Methods 5:296–308

Osburn CL, Rudolph JC, Paerl HW, Hounshell AG, Van Dam BR (2019) Lingering carbon cycle effects of Hurricane Matthew in North Carolina's coastal waters. Geophys Res Lett 46:2654–2661

Powley HR, Polimene L, Torres R, Al Azhar M, Bell V, Cooper D, Artioli Y (2024) Modelling terrigenous DOC across the north west European Shelf: fate of riverine input and impact on air-sea CO2 fluxes. Sci Total Environ 912:168938

Raymond PA, Bauer JE (2001) Riverine export of aged terrestrial organic matter to the North Atlantic Ocean. Nature 409(6819):497–500

Romera-Castillo C, Chen M, Yamashita Y, Jaffé R (2014) Fluorescence characteristics of size-fractionated dissolved organic matter: implications for a molecular assembly based structure? Water Res 55:40–51

Rudolph JC, Arendt CA, Hounshell AG, Paerl HW, Osburn CL (2020) Use of geospatial, hydrologic, and geochemical modeling to determine the influence of wetland-derived organic matter in coastal waters in response to extreme weather events. Front Mar Sci 7:18

Santos L, Pinto A, Filipe O, Cunha Â, Santos EB, Almeida A (2016) Insights on the optical properties of estuarine DOM–hydrological and biological Influences. PLoS ONE 11(5):e0154519

Singh S, Inamdar S, Mitchell M, McHale P (2014) Seasonal pattern of dissolved organic matter (DOM) in watershed sources: influence of hydrologic flow paths and autumn leaf fall. Biogeochemistry 118:321–337

Spencer RG, Aiken GR, Wickland KP, Striegl RG, Hernes PJ (2008) Seasonal and spatial variability in dissolved organic matter quantity and composition from the Yukon River basin, Alaska. Glob Biogeochem Cycles. https://doi.org/10.1029/2008GB003231

Stedmon CA, Markager S (2001) The optics of chromophoric dissolved organic matter (CDOM) in theGreenland Sea: An algorithm for differentiation between marine and terrestrially derived organic matter. Limnologyand Oceanography 46(8):2087–2093

Stedmon CA, Markager S, Søndergaard M, Vang T, Laubel A, Borch NH, Windelin A (2006) Dissolved organic matter (DOM) export to a temperate estuary: seasonal variations and implications of land use. Estuar Coasts 29:388–400

Uher G, Hughes C, Henry G, Upstill-Goddard RC (2001) Non-conservative mixing behavior of colored dissolved organic matter in a humic-rich, turbid estuary. Geophysical Research Letters 28(17):3309–3312

Van de Broek M, Vandendriessche C, Poppelmonde D, Merckx R, Temmerman S, Govers G (2018) Long-term organic carbon sequestration in tidal marsh sediments is dominated by old-aged allochthonous inputs in a macrotidal estuary. Glob Chang Biol 24:2498–2512

Virtasalo J, Österholm P, Asmala E (2023) Estuarine flocculation dynamics of organic carbon and metals from boreal acid sulphate soils. Biogeosci Discuss 2023:1–32

Ward ND, Megonigal JP, Bond-Lamberty B, Bailey VL, Butman D, Canuel EA, Windham-Myers L (2020) Representing the function and sensitivity of coastal interfaces in Earth system models. Nat Commun 11:2458

Zhao L, Gao L, Thomas DN (2024) Molecular size variations of chromophoric dissolved organic matter (CDOM) along a salinity gradient in the Changjiang River estuary. Estuar Coast Shelf Sci 297:108606

Zsolnay A, Baigar E, Jimenez M, Steinweg B, Saccomandi F (1999) Differentiating with fluorescence spectroscopy the sources of dissolved organic matter in soils subjected to drying. Chemosphere 38:45–50

Publisher's Note Springer Nature remains neutral with regard to jurisdictional claims in published maps and institutional affiliations.